Optical Materials 32 (2010) 1389–1392

Contents lists available at ScienceDirect

Optical Materials

journal homepage: www.elsevier.com/locate/optmat

Formation of Nd^{3+} doped Strontium Barium Niobate nanocrystals by two different methods

P. Haro-González *, L.L. Martín, S. González-Pérez, I.R. Martín [1]

Dep. Física Fundamental, Electrónica y Sistemas, Universidad de La Laguna, Av. Astrofísico Francisco Sánchez, s/n, E-38206 La Laguna, Tenerife, Spain

ARTICLE INFO

Article history:
Received 3 November 2009
Accepted 26 March 2010
Available online 18 April 2010

Keywords:
Strontium Barium Niobate
Nd^{3+}
Laser irradiation

ABSTRACT

The study of two different methods to obtain Strontium Barium Niobate nanocrystals has been carried out. Previously, Nd_2O_3 doped $SrO–BaO–Nb_2O_5–B_2O_3$ glasses were fabricated using the melt quenching process. In the first method, a thermal treatment in an electrical furnace at 620 °C was used to obtain glass ceramic samples. In the second one, the nanocrystals were obtained under continuous Ar laser irradiation in a localized zone in the glass sample. The X-ray diffraction patterns confirmed the formation of SBN nanocrystals in both cases. The optical measurements indicate the incorporation of Nd^{3+} ions into the nanocrystals which produces an increment of the luminescence intensity. Moreover, a calibration with the temperature has been carried out for the ratio of the Nd^{3+} emissions. This result could let to control the temperature of the laser irradiated zone.

1. Introduction

Glasses having high transparency, high chemical durability, excellent thermal and electrical properties are key materials in microelectronics, optics, and optical fiber technology. Micro-fabrication of glass materials has found increasingly more applications in optoelectronics, telecommunications, and photonic devices such as optical gratings and waveguides, and laser irradiation to glass has received considerable attention as a new tool of spatially selected micro-fabrication [1–5].

The good electro-optical and non-linear optical properties of $Sr_{1-x}Ba_xNb_2O_6$ (SBN) make it a very interesting crystal for technological application like frequency doubling, optical parametric oscillation and optical storage of information [6–9]. SBN is an attractive material being widely considered very useful in diverse device applications. It has been shown that by doping rare-earth and alkali ions into SBN crystals, substantially enhanced electro-optic and photorefractive coefficients can be obtained. For this reason there is a big interest in fabricating high quality rare-earth/alkali ions doped SBN [10]. Recently, SBN has been doped with optically active ions to investigate their applications in the field of photorefractive memories and self frequency converter solid state laser materials [11–13].

The aim of this work is the study of the formation of Nd^{3+}-doped SBN nanocrystals by two different ways. First, using the conventional crystallization in an electric furnace and second, inducing crystallization by laser irradiation. Optical measurements are reported to compare both methods.

2. Experimental

The $Nd_2O_3–SrO–BaO–Nb_2O_5–B_2O_3$ glasses are prepared using the melt quenching method with a composition of 5 Nd_2O_3, 11.25 SrO, 11.25 BaO, 22.5 Nb_2O_5, and 50 B_2O_3 in mol%. Commercial powders of reagent grade are mixed and melted in a platinum crucible for 1 h in an electric furnace at 1400 °C. The melt is poured between two iron plates and the thickness of the sample is 0.7 mm. The sample is polished to obtain a smooth and flat surface in both faces, and this makes sure that the laser does not diverge when irradiates the sample.

To obtain nanocrystals by conventional treatment, the sample is heated at 620 °C for 2 h. Respect to obtain nanocrystals by laser irradiation, a cw Ar-laser is used to devitrify a small area increasing the laser power beam from 0.4 to 1.5 W. In order to reach the smallest irradiated area, the laser beam is focused on the glass sample with a convergent lens. Simultaneously to the desvitrification process, it is measured the emission band of the $^4F_{3/2} \rightarrow {}^4I_{9/2}$ transition at 880 nm. These measurements are carried out with an Ocean-Optic High-Resolution Spectrometer.

The beam profile was measured, and a Gaussian profile with a width at half height of 1.4 mm was obtained. The laser beam was

* Corresponding author. Address: Universidad de La Laguna, Facultad de Física, Departamento de física fundamental y experimental, electrónica y sistemas, 38206, La Laguna, S/C de Tenerife, Spain. Tel.: +34 922 318651; fax: +34 922 318228.
E-mail addresses: patharo@ull.es (P. Haro-González), imartin@ull.es (I.R. Martín).
[1] MALTA Consolider Team.

0925-3467/$ - see front matter © 2010 Elsevier B.V. All rights reserved.
doi:10.1016/j.optmat.2010.03.011

focalized on the sample using a 100 mm focal lens. The diameter of the focalized spot d_1 is given by the formula:

$$d_1 = \frac{\lambda f}{\pi d_2} \quad (1)$$

where λ is the excitation wavelength, f the focal of the lens and d_2 the diameter of the collimated pumping beam before the lens. A mean diameter of about 11 μm is obtained for the pump spot on the sample. Therefore, at the maximum power in this experiment, 1.5 W, it can be obtained an energy fluence of about 0.4 mW/cm^2.

After this heating process, the emission spectra are obtained at low power excitation in order to appreciate the changes produced in the $^4F_{5/2} \rightarrow {}^4I_{9/2}$ and $^4F_{3/2} \rightarrow {}^4I_{9/2}$ transitions in the heat treated sample and inside the irradiated area by laser irradiation.

3. Results and discussion

As it was mentioned previously, the bulk glass ceramics samples doped with Nd^{3+} ions have been obtained using an electric furnace after a heat-treatment of 2 h at 620 °C. The formation on nanocrystals into the glass matrix is based in two steps: a nucleation process and crystal growth process. These samples have been checked analyzing the XDR patterns (see Fig. 1). These results shown that precursor glass pattern is completely amorphous with no diffraction peaks of crystals. After the heat-treatment, several broad peaks appeared, all of which are attributed to SBN crystalline phase. From the obtained peak widths of XRD pattern, the crystal size of SBN was estimated by using Sherrer's equation [14]. The average size of the precipitated SBN nanocrystals has been estimated to be around 60 nm.

In other way, a local area of Strontium Barium Niobate glass doped with Nd^{3+} has been irradiated using an Argon laser increasing the laser power beam from 0.4 to 1.5 W. This zone is heated to a high temperature which induces the nucleation and growth of Nd^{3+} doped nanocrystals near to the focal point. The formation of nanocrystals in this zone due to the laser action has been also confirmed by XDR measurements (see Fig. 1) and with a similar average size than those obtained under thermal treatment in a furnace (around 60 nm). In other matrix has been demonstrated other crystallization processes due to the irradiation with laser [15,16].

In the laser irradiation method the heating is due to the energy absorbed by the matrix or/and the optically active ions. Respect to the precursor glass matrix, it is very transparent in the range of the multiline argon laser. Therefore, the irradiation energy is principally absorbed by Nd^{3+} ions, which have absorptions bands coincident with the output wavelengths of the laser. In this situation the Nd^{3+} ions are excited from the ground state to upper levels, from which relax non-radiatively to the $^4F_{3/2}$ level. Therefore, the local temperature rises in the focal point of the laser beam. In general, under this process the temperature of Ar:Laser irradiated zone in glass depends on the amount of Nd^{3+} ions, laser power, laser irradiation time, specific heat and thermal conductivity of the matrix. This temperature results in higher local phonon density and in a more efficient non-radiative decay of photoexcited Nd^{3+} ions and in a more efficient heating. This process has been reported by other authors in a different matrix doped with Er^{3+} ions under pulsed femtosecond laser irradiation [17].

During the irradiation process, the emission bands of the $^4F_{5/2} \rightarrow {}^4I_{9/2}$ and $^4F_{3/2} \rightarrow {}^4I_{9/2}$ transitions have been measured in order to determinate when the desvitrification is completed. The spectra at low and high power excitation are given in Fig. 2. When the sample is irradiated, the $^4F_{3/2}$ level is populated giving to place the $^4F_{3/2} \rightarrow {}^4I_{9/2}$ transition, centered at 880 nm. As the laser power pump increases, the intensity of this transition also increases. Moreover, in the Fig. 2, it is shown a weak peak centered at 810 nm which corresponds to the $^4F_{5/2} \rightarrow {}^4I_{9/2}$ transition. When the pumping power increases, the ratio between these bands changes due to the rise of temperature on the focalized zone, allowing the $^4F_{5/2}$ level to be thermally populated from $^4F_{3/2}$. The evolution of these intensities changes while the irradiated power is increased as can be seen in the inset. Initially, the 810 nm peak is clearly smaller than the 880 nm due to the low power excitation. When the irradiation intensity increases, the emission band at 810 nm starts to growth faster than the 880 nm peak until they reach the same intensity value at about 1200 mW. At 1300 mW, there is a change in the slope which could be an indicative that the structure of the sample has changed. At the end of this process, it is obtained a desvitrificated zone of 300 μm. The size of this area is longer than the focalized laser spot (about 11 μm), it could be explained due to the continuous regimen of the laser excitation which produce a temperature gradient on the sample surface (from the spot center to the border).

In order to check the temperature of the sample as a function of the laser power, it is interesting to study the thermalization of the

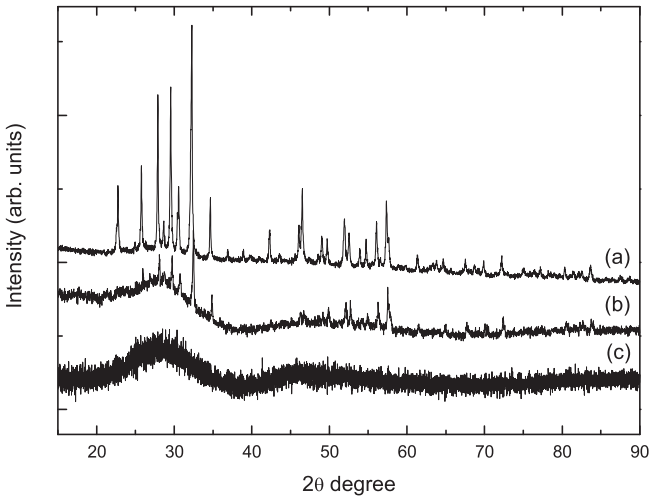

Fig. 1. XRD patterns of the sample obtained by thermal treatment (a), by laser irradiation (b) and the glass precursor (c).

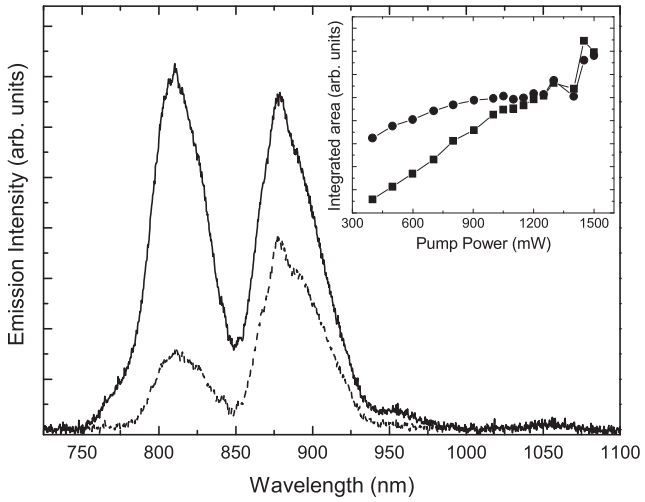

Fig. 2. Emission fluorescence spectra obtained for a irradiated local area of an SBN glass doped with 5% of Nd^{3+} using an Argon laser at low (400 mW – dashed line) and high (1500 W – straight line) power excitation. Inset-integrated area of the two intensity peaks obtained in the emission fluorescence spectra while increasing the laser power beam until 1500 mW. The circle symbols correspond to the area at 880 nm, whereas the square symbols, to the 810 nm.

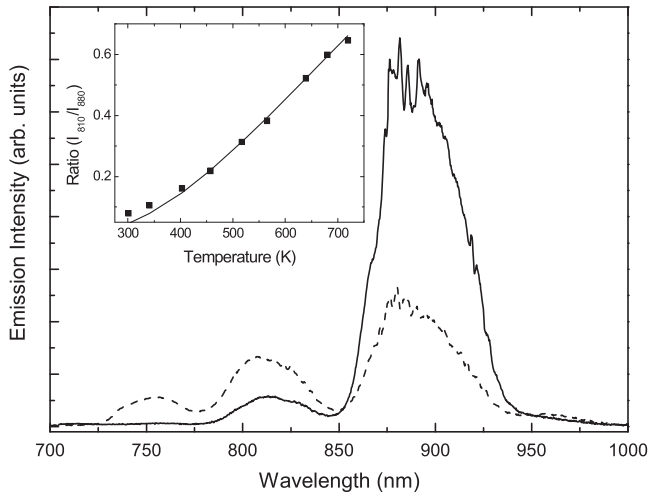

Fig. 3. Emission fluorescence spectra of the glass precursor inside an electric furnace at 300 K (straight line) and 680 K (dashed line). The inset shows the intensity ratio of the 810 nm (squares) and 880 nm (circles) emission bands as a function of the temperature. The straight line is the fit to the equation, as explained in the text.

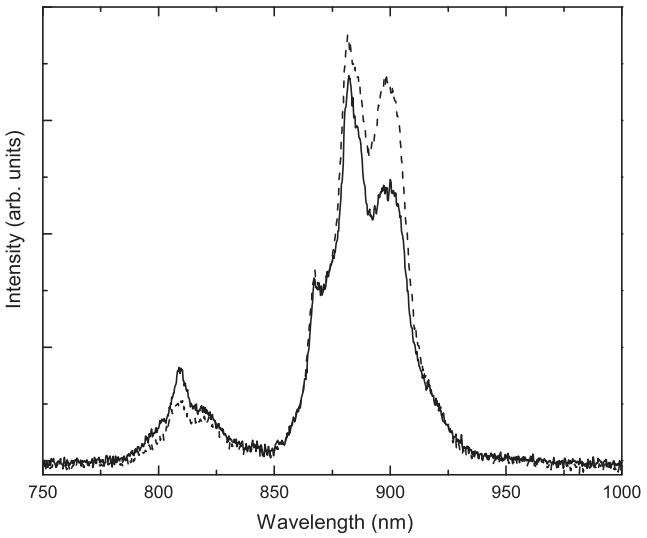

Fig. 4. Emission fluorescence spectra obtained after exciting with an Argon laser the glass ceramic sample (dashed line) and inside the irradiated area (straight line).

$^4F_{5/2}$ and $^4F_{3/2}$ levels. An analysis based on a simple three-level system comprised of the $^4F_{5/2}$ (level 3), $^4F_{3/2}$ (level 2) and $^4I_{9/2}$ (level 1) has been carried out. The ratio between the intensities of the areas at 810 nm ($^4F_{5/2} \rightarrow {}^4I_{9/2}$) and 880 nm ($^4F_{3/2} \rightarrow {}^4I_{9/2}$) can be related to the temperature T as:

$$\frac{I_{31}}{I_{21}} = \frac{\omega_{31}^R g_3 h\nu_3}{\omega_{21}^R g_2 h\nu_2} \exp\left(\frac{-E_{32}}{KT}\right) \quad (2)$$

where K is the Boltzmann constant, E_{32} is the energy gap between these two excited levels, g_3, g_2 are the degeneracies $(2J+1)$ of the levels, ω_R^{31} and ω_R^{21} are the spontaneous emission rates of the $^4F_{5/2}$ and $^4F_{3/2}$ levels to the $^4I_{9/2}$ level, respectively. This relation was checked by recording the emission spectra at different temperatures from 300 to 720 K for the glass sample. Therefore, the sample was introduced in a furnace in order to control its temperature. As example, the emission intensity spectra at room temperature (300 K) and at high temperature (680 K) are shown in Fig. 3. The inset gives the obtained result of the intensities ratio of both peaks versus temperature. The ratio (I_{810}/I_{880}) increases with the temperature as $^4F_{5/2}$ level is populated. From the least-squares fit to Eq. (2), the value of the energy gap between the two levels was found to be 953 cm^{-1} and the pre-exponential factor 4.4.

From the intensity ratio of these emission bands (I_{810}/I_{880}) and the values obtained by calibrating these emissions with the sample in an electric furnace, it can be estimated the temperature. At the laser power of 1.3 W, where there is a change in the slope of the emission intensities (see inset of Fig. 2), could be estimated a temperature for the sample about 920 K. This result is in good agreement with the obtained for the glass ceramic sample where the temperature used for the thermal treatment is 900 K. This fact allows concluding that the laser irradiation induced a phase transition on the sample where it has passed from a glassy to a crystalline phase. Therefore, it is obtained the threshold for the excitation power in this experimental setup at 1.3 W.

After the irradiation process, the emission spectrum is obtained at low power excitation in order to appreciate the changes produced in the $^4F_{3/2} \rightarrow {}^4I_{9/2}$ transition. As can be seen in Fig. 4, the emission bands reveals sharp sub-band structure due Stark splitting which is generally obtained in a crystal host [18] and it is similar to the spectrum obtained for the glass ceramics sample. This result confirms that the Nd^{3+} ions have been incorporated into the SNB nanocrystals after the irradiation process. However, the spectrum of the glass sample shows a broad band without structure, which is characteristic of glassy phase (as can be seen in Fig. 2). Therefore, the rest of Nd^{3+} ions which reside in the glassy phase in the glass ceramic sample or in the irradiated area could produce the difference in the spectra shown in Fig. 2.

4. Conclusions

A study of crystallization made by standard thermal treatment and laser heating on a 5 mol% Nd^{3+} doped SBN glass has been carried out. To obtain SBN nanocrystals, the precursor glass, fabricated using the melt quenching method, was heating by standard thermal treatment in an electric furnace at 620 °C or was irradiated under continuous Ar laser from 0.4 to 1.5 W. The X-ray diffraction patterns confirmed the formation of SBN nanocrystals in both cases.

The optical measurements were carried out and indicated the incorporation of Nd^{3+} ions into the nanocrystals which produces an increment of the luminescence intensity. Moreover, it is shown that analyzing the intensity ratio of the emissions at 810 and 880 nm is possible to estimate the temperature of the sample during laser irradiation. This temperature control process could let to obtain a localized zone in the sample with Nd^{3+} doped nanocrystals.

Acknowledgments

The authors gratefully acknowledge the financial support of this research by the Comisión Interministerial de Ciencia y Tecnología (MAT-2007-63319 and MAT-2007-65990-C03-02), Malta Consolider-Ingenio 2010 (CSD2007-0045) and FPI grant by Agencia Canaria de Investigación del Gobierno de Canarias.

References

[1] K.O. Hill, B. Malo, F. Bilodeau, D.C. Jhonson, J. Albert, Appl. Phys. Lett. 62 (1993) 1035–1037.
[2] D. Du, X. Liu, G. Korn, J. Squier, G. Mourou, Appl. Phys. Lett. 64 (1994) 3071–3073.
[3] K.M. Davis, K. Miura, N. Sugimoto, K. Hirao, Opt. Lett. 21 (1996) 1729–1731.
[4] T. Fujiwara, T. Nakamoto, T. Honma, Y. Benino, T. Komatsu, Electron. Lett. 39 (2003) 1576–1577.
[5] H. Ebendorff-Heidepriem, Opt. Mater. 25 (2004) 109–115.
[6] H. Liu, S.T. Li, F.E. Fernandez, G.K. Liu, Thin Solid Films 424 (2003) 61–65.

[7] T. Volk, D. Isakov, V. Salobutin, L. Ivleva, P. Lykov, V. Ramzaev, M. Wöhlecke, Solid State Commun. 130 (2004) 223–226.
[8] N. Chayapiwut, T. Honma, Y. Benino, T. Fujiwara, T. Komatsu, J. Solid State Chem. 178 (2005) 3507–3513.
[9] T.P.J. Han, Jaque D. Jaque, J. García-Sole, L. Ivleva, J. Lumin. 119–120 (2006) 453–456.
[10] Z.R. Shen, H. Ye, C.L. Mak, T.Y. Yum, K.H. Wong, Thin Solid Films 515 (2007) 3475.
[11] M. Bettinelli, A. Speghini, A. Rodenas, P. Molina, M.O. Ramirez, B. Capote, D. Jaque, L.E. Bausa, J. Garcia-Sole, J. Lumin. 122–123 (2007) 307–310.
[12] P. Haro-González, F. Lahoz, J. González-Platas, J.M. Cáceres, S. González-Pérez, D. Marrero-López, N. Capuj, I.R. Martín, J. Lumin. 128 (2008) 908–910.
[13] P. Haro-González, S. González-Pérez, I.R. Martin, F. Lahoz, N.E. Capuj, D. Jaque, Appl. Phys. A 93 (2008) 977–981.
[14] P. Klug, L.E. Alexander, X-ray Diffraction Procedure, Wiley, New York, 1954 (Chapter 9).
[15] V.P. Veiko, Q.K. Kiev, N.V. Nikonorov, V.Ya. Shur, A. Luches, S. Rho, Appl. Surf. Sci. 248 (2005) 231–237.
[16] Y. Shimotsuma, K. Hirao, J. Qiu, K. Miura, J. Non-Cryst. Solids 352 (2006) 646–656.
[17] V.K. Tikhomirov, A.B. Seddon, J. Koch, D. Wandt, B.N. Chichkov, Phys. Status Solidi A 202 (2005) R73.
[18] J.J. Romero, D. Jaque, L.E. Bausá, A.A. Kaminskii, J. García Solé, J. Lumin. 87–89 (2000) 877–879.